

# An Improved Wavefront Reconstruction Method for Breast Microwave Imaging

Daniel Flores-Tapia, Gabriel Thomas, Stephen Pistorius

**Abstract-** Breast cancer is the leading cause of cancer related deaths in women between the ages of 15 and 54, and the second cause of cancer death in women the 55 to 74 age range. In recent years, Breast Microwave Imaging (BMI) has shown its potential as a promising breast cancer detection technique. This imaging technology is based on the electrical characteristic differences that exist between normal and malignant breast tissues at the microwave frequency range. A novel reconstruction approach for the formation of 2D BMI models is proposed in this paper. This technique uses the phase differences introduced during the collection of target responses in order to determine the correct spatial location of the different structures that constitute the final image. The proposed method yielded promising results when applied to simulated data sets obtained from Magnetic Resonance Images (MRI).

## I. INTRODUCTION AND MOTIVATION

During the last decade, the use of microwave techniques as a complimentary tool for breast cancer detection has been proposed [1,2,3,4]. The basis of this imaging modality are the dielectric differences between cancer and normal breast tissue in the 900MHz-20GHz frequency range[5]. One of the most promising microwave technologies for breast cancer detection is Breast Microwave Radar Imaging (BMRI). Similarly to conventional radar applications, BMRI systems irradiate an electromagnetic wave into the scan area, which is usually formed by several types of tissues with different dielectric properties. The backscattered signals from the different breast structures are then recorded and displayed so they can be visualized and interpreted.

The BMRI data acquisition process is performed along circular or quasi circular scan trajectories in order to suit better the geometry of the breast region. As discussed in [3], as the irradiation is performed along the scan trajectory, the target responses have different travel times, resulting in the formation of non linear signatures. This fact makes difficult to determine the correct dimensions and locations of the different scattering structures present in the scan area.

In order to properly visualize the targets reflections, the collected data must be focused [6]. During the last years, a Manuscript received on April,7,2009. This work was supported by CancerCare Manitoba, MITACS, the Natural Sciences and Engineering Research Council of Canada and the University of Manitoba

Daniel Flores-Tapia and Stephen Pistorius are with the Department of Medical Physics, CancerCare Manitoba, Winnipeg, Manitoba, R3E 0V9, Canada, (email: daniel.florestapia, stephen.pistorius@cancercare.mb.ca).

Gabriel Thomas are with the Electrical and Computer Engineering Department, University of Manitoba, Winnipeg, Manitoba, R3T 5V6 Canada (phone: (204) 474-6893, fax: (204) 261-4639, e-mail: thomas@ee.umanitoba.ca).

wide variety of techniques have been proposed for BMRI reconstruction purposes. In general, these methods can be classified as either time-shift techniques or wavefront reconstruction approaches. Time-shift techniques perform a shift-sum process over a set of focal points in the scan area. Two examples of this approach are the confocal mapping algorithm [3,4] and the beamforming reconstruction method [2].

The use of wavefront reconstruction techniques to form BMRI images has been proposed by the authors in [6]. Wavefront reconstruction approaches focus the data by processing the spectrum of the collected reflections and transferring it from the spatial-temporal domain where it is originally acquired to the spatial domain where it will be displayed. Although each method has advantages and disadvantages of their own, time-shift techniques are characterized by their low computational cost, while wavefront reconstruction approaches exhibit a higher Signal to Noise Ratio (SNR) and an increased focus quality [6].

A problem of wavefront reconstruction approaches is their execution time. Depending on the sampling parameters of the radar system, the time needed to form an image is between 12.5 seconds to 2 minute. In this paper, an improved wavefront reconstruction technique is proposed. This approach uses a novel interpolation approach to significantly reduce the image reconstruction time without compromising the focal quality and noise levels of the focused images. The proposed method was evaluated using a set of numeric phantoms obtained from Magnetic Resonance Imagery (MRI) data sets. The execution time, SNR and focal quality of the reconstructed images was calculated in order to assess the performance of the proposed technique.

This paper is organized as follows. The signal model is described in section 2. In section 3, a description of the proposed approach is given. The results of the proposed reconstruction technique using simulated data are shown and discussed in section 4. Finally, concluding remarks can be found in section 5.

## II. SIGNAL MODEL

A 2D cylindrical scan trajectory is used in this paper. In this approach, the patient lies in a prone position and the antenna array is positioned in a circular array in the  $x$ - $y$  plane around the circular shape adopted by the breast [6]. Let consider a circular array formed by  $N$  antennas uniformly distributed in a circle of radius  $R$ . In this case, every element is facing towards the center of the array.  $T$  point scatterers are assumed to be located inside the area

delimited by the array. For the following discussion, the center of the antenna array will be considered to be at the origin of the coordinate system. Also, a polar coordinate system will be used in order to simplify the calculations. Then, the location of the  $p$  scatter will be  $(r_p, \phi_p)$  where  $r_p = \sqrt{x_p^2 + y_p^2}$  and  $\phi_p = \tan^{-1}(y_p/x_p)$ . In this case the distance between the scan location at  $(R, \theta)$  and the  $p$  scatter is  $D = \sqrt{R^2 + r_p^2 - 2 \cdot R \cdot r_p \cos(\phi_p - \theta)}$ . A diagram of this model can be seen in figure 1.

At each scan location, on at a time, a waveform  $f(t)$  is radiated and the responses from the targets with the scan area are recorded at the same scan position. For the scan location at  $(R, \theta)$ , the received signal can be expressed as:

$$s(t, \theta) = \sum_{q=1}^T \sigma_j f\left(t - \frac{2\sqrt{R^2 + r_q^2 - 2 \cdot R \cdot r_q \cos(\phi_q - \theta)}}{\nu}\right). \quad (1)$$

where  $\nu$  is the propagation speed of the medium and  $\sigma_j$  is the reflectivity of the  $q^{\text{th}}$  target. The collected data set is a function of the signal travel time and the spatial location of the recording point.

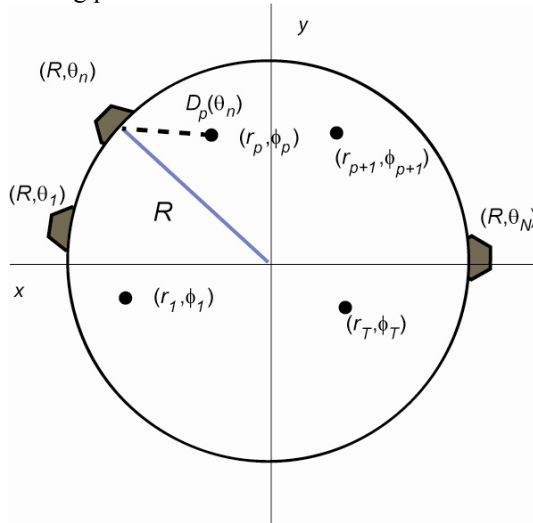


Figure 1. Geometry of the cylindrical array

### III. FAST WAVEFRONT RECONSTRUCTION

Due to the fact that most of the BMRI data is acquired and processed using digital equipment,  $s(t, \theta)$  usually has the form of an evenly sampled discrete space. This is. The sampled version of  $s(t, \theta)$ , is defined over an  $L \times N$  grid, where  $L$  is the number of time samples,  $N$  is the total scan locations in the circular scan pattern. Wavefront reconstruction techniques transfer the spectrum of the collected data from its original spatial temporal frequency space to the spatial frequency space corresponding to the scan area. The first step to accomplish this is to calculate the Fourier transform of the collected data in the  $t$  and  $\theta$  scan trajectories. This resulting expression is:

$$\begin{aligned} S(\omega, \varepsilon) &= \sum_{q=1}^T 4\sigma_q F(\omega, \varepsilon) \\ &\cdot \exp\left(-j\left(\varepsilon \cdot \left(\sin^{-1}(\varepsilon/2kR) + \sin^{-1}(\varepsilon/2kr_p) + \pi + \phi_p\right)\right)\right) \end{aligned} \quad (2)$$

where  $F(\omega, \varepsilon)$  is the spectrum amplitude component in the  $(\omega, \varepsilon)$  frequency space. Details about the mathematic procedure behind the derivation of (2) can be found in [6].

The spectrum of the spherical phase function is formed by two main components. The first type, denoted as  $\kappa_p(\omega, \varepsilon', k'_z)$ , are the Phase Modulated (PM) terms related to the target responses. These terms are a function of the target location,  $(r_p, \phi_p)$ . The second type of spectral components,  $\chi(\omega, \varepsilon', k'_z)$ , are the PM terms related to the delays produced by the shape of the scan geometry. In order to eliminate the effects of the scan trajectory on the collected data,  $\chi(\omega, \varepsilon', k'_z)$  must be removed from  $S_p(\omega, \varepsilon', k'_z)$ . For this purpose, the following operation is performed:

$$U(\omega, \varepsilon) = S(\omega, \varepsilon) \cdot C(\omega, \varepsilon) \quad (3)$$

where  $\varepsilon$  is the frequency counterpart of  $\theta$  and:

$$C(\omega, \varepsilon) = \exp\left(j\left(\sqrt{4k^2R^2 - \varepsilon^2} + \varepsilon \cdot (\sin^{-1}(\varepsilon/2kR) + \pi)\right)\right) \quad (4)$$

A detailed explanation about the derivation of the expression corresponding to  $C(\omega, \varepsilon)$  can be found in [6]. Next, the inverse Fourier transform of the compensated data in the  $\varepsilon$  direction is calculated. The resulting expression is:

$$S_c(\omega, \theta) = \sum_{q=1}^T \sigma_q \zeta(\omega, \theta) \cdot \exp(-j(2kr_j \cos(\theta - \phi_j))) \quad (5)$$

where  $k = \omega/\nu$  is often called the wavenumber.

According to the Fourier slice theorem,  $S(\omega, \theta)$  corresponds to a set of  $M$  equally spaced projections of the rectangular frequency spectrum,  $I(k_x, k_y)$ , of the target responses. Each projection passes through the origin and has the same angle that the scan locations where it was recorded. To be able to visualize the compensated data in a rectangular coordinate system,  $S(\omega, \theta)$  must be transferred to the frequency space  $(k_x, k_y)$ . Usually this is done using the following mapping:

$$k_{ix} = m/\nu \cdot \cos(n), \quad k_{iy} = m/\nu \cdot \sin(n) \quad \forall (m, n) \in (\omega, \theta). \quad (6)$$

The problem with this mapping is that the separation between the adjacent samples is not uniform. Although this kind of frequency spaces can be processed using Fourier techniques that consider non equidistant sampling, the resulting images exhibit reduced spatial resolution and the formation of ringing artifacts. If conventional Fourier techniques are to be used, an interpolation process must be performed to generate an evenly sampled spectrum. The interpolation in these cases is often done by using Qhull based interpolation methods [7]. However, these approaches have an expected performance of  $O(n \cdot \log(n))$ , which in BMRI applications results in execution times of 35 seconds to 1 minute per image when executed on a conventional PC[6,7]. An alternate way is to generate  $(k_x, k_y)$  using a look-up table approach. This kind of interpolation approaches are used to determine intermediate values within the data points in an evenly sampled interpolation grid. Due to the distance between adjacent samples, this approach can be applied on  $S_c(\omega, \theta)$ . In order to generate  $I(k_x, k_y)$ , first lets define the discrete  $N \times N$  frequency space  $(k_x, k_y)$  such as:

$$k_y = k_x \triangleq \{n\pi/R \mid n \in Z \text{ and } -N \leq n \leq N\}. \quad (7)$$

Next, we calculate the functions  $k_r(p, q)$  and  $\vartheta(p, q)$  as follows:

$$k_r(p, q) = \sqrt{p^2 + q^2}$$

$$\vartheta(p, q) \begin{cases} \tan^{-1}(q/p) & \text{if } p > 0 \text{ and } q \geq 0 \\ \tan^{-1}(q/p) + 2\pi & \text{if } p < 0 \text{ and } q \geq 0 \\ \tan^{-1}(q/p) + \pi & \text{if } p < 0 \\ \frac{\pi}{2} & \text{if } p = 0 \text{ and } q > 0 \\ \frac{3\pi}{2} & \text{if } p = 0 \text{ and } q < 0 \end{cases} \quad (8)$$

$$\forall (p, q) \in (k_x, k_y).$$

At this point, we can define the auxiliary discrete frequency space  $(\rho, \varphi)$  where  $\rho$  and  $\varphi$  are the ranges of  $k_r(p, q)$  and  $\vartheta(p, q)$  respectively. Now the values of  $S_c(\omega, \theta)$  at the points contained in  $(\rho, \varphi)$  can be calculated by using a conventional interpolation approach. This set of values will be denoted as  $S_c(\rho, \varphi)$ . Next, we can map  $S_c(\rho, \varphi)$  into  $(k_x, k_y)$  using the following function:

$$I(\alpha(u, v), \beta(u, v)) = S_c(u, v) \quad (9)$$

where:

$$\begin{aligned} \alpha(u, v) &= u \cos v \\ \beta(u, v) &= u \sin v \\ \forall (u, v) &\in (\rho, \varphi). \end{aligned} \quad (10)$$

Since (10) is the inverse of the mapping process described in (8), and both relations have a one to one relation, it is not difficult to prove that the  $\alpha(u, v)$  and  $\beta(u, v)$  map the points in  $(\rho, \varphi)$  back into  $(k_x, k_y)$ , therefore  $I(\alpha(u, v), \beta(u, v))$  can be also regarded as  $I(k_x, k_y)$  and it does not have any gaps within its spectral support band. Therefore the relation expressed in (9) results in an

evenly sampled spectrum with no gaps in the support band. Finally, in order to visualize the reconstructed data in the spatial domain a 2D inverse FFT is applied to  $I(k_x, k_y)$ . The result of this process is the reconstructed image  $i(x, y)$ .

#### IV. RESULTS

In order to assess the capabilities of the proposed method, a set of simulated data was produced using a radar simulator developed by the authors [8]. This data was generated using a simulated pattern of 72 scan locations with a 0.4m radius in the  $x$ - $y$  plane. MRI data sets were used to generate the numeric phantoms. These data sets were obtained from the University of Wisconsin-Madison online phantom repository. The dielectric properties of the breast regions contained in the MRI data sets were determined using the values published in [5]. A Stepped Frequency Continuous Wave (SFCW) was used as the irradiated signal. The SCFW had a bandwidth of 11 GHz with a center frequency of 6.5 GHz. The proposed method was implemented in a desktop PC with a 2.6 Ghz Phenom 9950 Quad CPU and 8 GB RAM. The proposed technique was implemented, tested and validated using a MATLAB development environment. The performance of the proposed method was quantitatively measured using two metrics, Signal to Noise Ratio (SNR) and conditional entropy. The SNR of the reconstructed images technique was calculated as follows:

$$SNR = 20 \cdot \log_{10} \left( \frac{\sum_{j=1}^T \Gamma_{j,3dB} / T}{\sigma^w} \right) \quad (11)$$

where  $\Gamma_{j,3dB}$  is the magnitude of the 3dB point of the  $j^{\text{th}}$  target signature in the image reconstructed by the proposed algorithm and  $\sigma^w$  is the standard deviation of the background noise. In this paper, the reflections from the fibroglandular tissue areas were not considered as noise due to the fact that these regions can provide anatomical information for post-reconstruction processing, i.e. image fusion. In each experiment, two data sets of the numeric phantom, one with a tumor and another without it, were generated. This was done to better visualize the effect of the tumor responses in the reconstructed images. To properly compare the performance of the proposed method with respect to current wavefront reconstruction approaches, which use a Qhull based interpolation procedure, the data set containing the tumor was also reconstructed using the technique proposed in [6]. A linear interpolation kernel was used in all the experiments.

The results of an initial experiment using the proposed method can be seen in figure 2. In this experiment, a tumor with a diameter of 5mm was inserted at  $(-0.02, -0.017)$  m. In order to have a better visualization of the reconstructed target responses, the surface reflections were removed using the method used by the authors in [6]. The red circle denotes the location of the removed skin reflections. A second numerical setup and its corresponding reconstructed images

are shown in figure 3. For this experiment, a tumor with a diameter of 5mm was inserted at (0.0125,-0.0025) m. Notice how in both cases the magnitude of the sidelobes is smaller than the image focused using the conventional wavefront reconstruction approach resulting in increased SNR values.

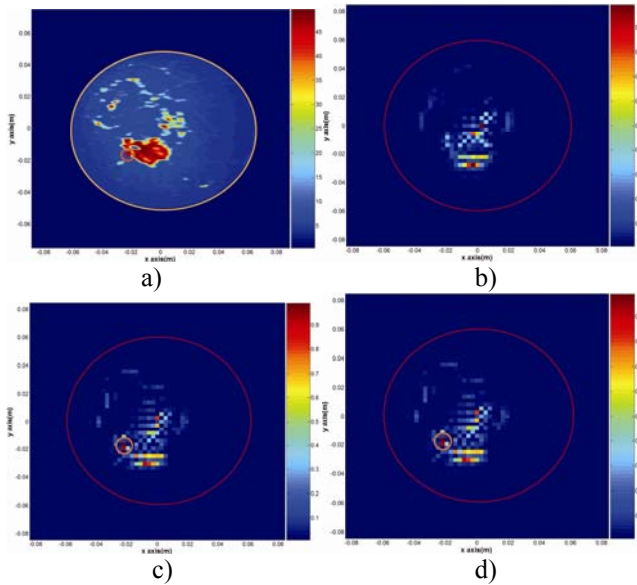


Figure 2. a) MRI model, b) Reconstructed image of the tumor-free data set, c) Reconstructed image obtained using the proposed approach, d) Reconstructed image using the conventional wavefront reconstruction approach. The tumor responses are encircled with an orange contour.

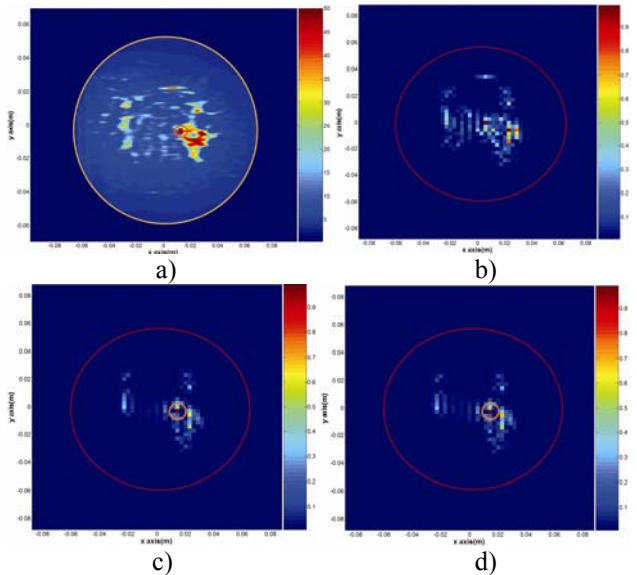


Figure 3. a) MRI model, b) Reconstructed image of the tumor-free data set, c) Reconstructed image obtained using the proposed approach, d) Reconstructed image using the conventional wavefront reconstruction approach. The tumor responses are encircled with an orange contour. The resulting SNR and conditional entropy values obtained in each experiment are summarized in Table I. Finally, the computational cost of the proposed technique was evaluated

by calculating the average execution time 30 simulated data sets. The average execution time was 1.25 seconds, compared to 35.4 seconds needed by the conventional wavefront reconstruction approach.

TABLE I  
SNR and Conditional Entropy value comparison in each experiment.

Technique/Experiment		SNR(dB)	Cond. Entropy (bits)
Conv. Wavefront	1	5.94	4.84
	2	9.84	4.63
Proposed Approach	1	6.04	1.58
	2	9.97	1.58

## V. CONCLUSION

A novel technique for 2D BMRI reconstruction was presented in this paper. Compared to conventional wavefront reconstruction techniques, the proposed approach uses a novel interpolation approach that results in shorter execution times and increased signal to noise ratio values and comparable focal quality. The proposed method yielded promising results when applied to simulated data generated from MRI data sets.

## REFERENCES

- [1] D. Li, P. M. Meaney and K. D. Paulsen "Conformal microwave imaging for breast cancer detection," *IEEE Transactions on Microwave Theory and Techniques*, vol. 51, pp. 1179-1185, April 2003.
- [2] Xu Li and S.C Hagness, "A confocal microwave imaging algorithm for breast cancer detection", *IEEE Microwave and Wireless Components Letters*, vol. 11, pp. 130 – 132, March 2001.
- [3] E. C. Fear and M. A. Stuchly, "Microwave detection of breast cancer," *IEEE Transactions on Microwave Theory and Techniques*, vol. 48, pp. 1854 – 1863, Nov. 2000.
- [4] M. Klemm, I. Craddock, J. Leendertz, A. Preece, R. Benjamin, "Experimental and clinical results of breast cancer detection using UWB microwave radar," *2008 IEEE Antennas and Propagation Society International Symposium*, vol. 1, no., pp.1-4, 5-11, July 2008.
- [5] M. Lazebnik, L. McCartney, D. Popovic, C. B. Watkins, M. J. Lindstrom, J. Harter, S. Sewall, A. Magliocco, J. H. Booske, M. Okoniewski, and S. C. Hagness, "A large-scale study of the ultrawideband microwave dielectric properties of normal breast tissue obtained from reduction surgeries," *Physics in Medicine and Biology*, vol. 52, pp. 2637-2656, April 2007.
- [6] D. Flores-Tapia, G. Thomas and S. Pistorius, "A wavefront reconstruction method for 3D cylindrical subsurface radar imaging," *IEEE Transactions on Image Processing*, vol. 17, pp. 1908-1925, October 2008.
- [7] V. Rasche, R. Proksa, R. Sinkus, P. Bornert, H. Eggers, "Resampling of data between arbitrary grids using convolution interpolation," *IEEE Transactions on Medical Imaging*, vol.18, pp.385-392, May 1999.
- [8] D. Flores-Tapia, G. Thomas, A. Sabouni, S. Noghianian, S. Pistorius, "Breast tumor microwave simulator based on radar signal model", *2006 IEEE International Symposium on Signal Processing and Information Technology*, vol. 1, pp 17-22, August 2006.